Numerical investigation and optimization of a mechano-optical sensor based on a grated waveguide optical cavity

S.V. Pham, L.J. Kauppinen, R.M. de Ridder and H.J.W.M. Hoekstra

Integrated Optical MicroSystems (IOMS) group, MESA+ Institute for Nanotechnology,
University of Twente, the Netherlands
s.v.pham@ewi.utwente.nl

Recently we have proposed and demonstrated a novel and compact read-out principle for cantilever deflection with a grated waveguide optical cavity. The device, consisting of a microcantilever suspended above a Si_3N_4 grated waveguide (GWG), is a potentially highly sensitive mechano-optical sensor for gas sensing. In this report, we present results of a numerical investigation to optimize such an integrated GWG-cantilever platform using the bidirectional eigenmode propagation method. The results show that sensitivity of the device strongly depends on the grating depth, length of the grated section and the cantilever width.

1. Introduction

Microcantilever-based sensors can be used to detect molecular absorption such as hydrogen gas, which causes changes in the surface stress [1-7], leading to deflection of the cantilever. Such a deflection can be determined by means of optical beam deflection [2], capacitance- [3], or piezo-resistance-[4] based readout. We have proposed a compact integrated mechano-optical sensor using a novel and highly sensitive integrated read-out scheme to detect small deflections of a cantilever in close proximity to a grated waveguide (GWG) structure [1,5,6]. In this paper, the sensitivity of such an integrated GWG-cantilever device is discussed. Based on the numerical simulations, a detailed calculation of the sensor performance is presented as a function of several parameters. The preliminary results provide general guidelines in choosing optimal device parameters. The rest of this paper is organized as follows. Section 2 describes the device structure, its sensing principle, and the most relevant parameters to be varied for optimization of the readout of cantilever deflection. In section 3 results are described and discussed. The paper ends with conclusions (section 4).

2. Device structure and parameters, and sensing principle

The 3D schematic structure and the cross-section of the GWG-cantilever device are shown in Figs.1a and 1b. Main parts of the device are the Si_3N_4 grated waveguide and the SiO_2 cantilever coated with a palladium functionalized layer for hydrogen absorption. All dimensions are depicted in the figure.

Absorption of H_2 into Pd will cause the cantilever to curl down [2-5], which narrows the GWG-cantilever gap, *g*, leads to stronger interaction between the cantilever and the GWG evanescent field, and results in a shift of the transmission spectrum. This effect can be used for the detection of cantilever displacements (see Fig. 1c).

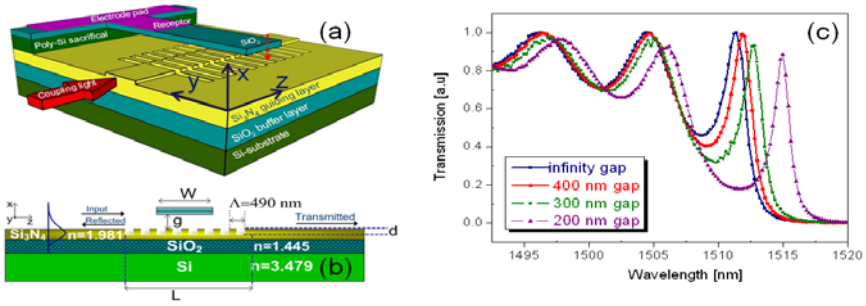

Fig. 1. The 3D schematic structure (a) and the cross-section (b) of the GWG-cantilever device, and the simulated spectral shift due to varying the GWG-cantilever gap

For sensing we use the (sharpest) first peak left of the bandgap, i.e., the peak at the right hand side of figure 1c. The sensitivity of the gas sensor, S, is given by

$$S \equiv \frac{\partial T}{\partial C} = S_{readout}\frac{\partial g}{\partial C} \;\; ; \;\; S_{readout} \equiv |\frac{\partial T}{\partial g}|, \qquad (1)$$

where T is the transmittance and C the gas concentration. In this work we focus on the optimization of the readout. The quantity $S_{readout}$ can be rewritten as

$$S_{readout} \equiv |\frac{\partial T}{\partial g}| = |\frac{\partial T}{\partial \lambda}\frac{\partial \lambda}{\partial g}|, \qquad (2)$$

where λ refers to the wavelength corresponding to the highest slope of $T(\lambda)$.

It can be argued, using eqs. 28 and 29 of chapter 2 of [7], that the 2nd quantity of the right hand side of the eq. 2 ($\partial\lambda/\partial g$) depends mainly on the modal field shape and the gap, g, according to

$$\frac{\partial \lambda}{\partial g} = \frac{\partial \lambda_p}{\partial g} \propto \; e^{-2\gamma g} \;, \qquad (3)$$

where λ_p refers to the wavelength of the peak maximum and γ is the decay constant along x (see Fig. 1a) of the most dominant field components of the grating mode. The factor $\partial T/\partial\lambda$ reflects the slope of the transmittance and depends mainly on the Q-factor of the cavity defined by the GWG-cantilever layout.

In this preliminary parameter research the following are fixed: thickness of the Si_3N_4 guiding layer (275 nm), period Λ of the grating (0.49 μm), and thickness of the cantilever (0.8 μm). Below we will investigate the device performance dependent on grating length (L) and depth (d), cantilever width (W) and GWG-cantilever gap (g) (see Table 1).

Table 1. Parameters used in the simulations (W=0 means that the device is a grating without a suspended cantilever)

Device	Grating length, L [μm]	Grating depth, d [nm]	Cantilever width, W [μm]	gap, g [nm]
A	125Λ	55	20	100-400
B	125Λ	75	20	100-400
C	125Λ	55	0-L	200
D	250Λ	55	0-L	200

4. Results and discussions

4.1. Fixed W=20 μm, varied L, d and g

Figure 2a shows 1st resonant wavelengths (left axis) and resonant-wavelength shifts (right axis) versus the gap between GWG and cantilever. The deeper grating (device B) results in a wider band gap and thus to a spectral shift to the left (see Fig.2a left axis). The quantity $\partial\lambda_p/\partial g$ is according to eq. 3 virtually independent of the grating depth and depends on g approximately as given by eq. 3 with γ=1/(200 nm), with $1/\gamma$ the approximate width of the evanescent tail of the

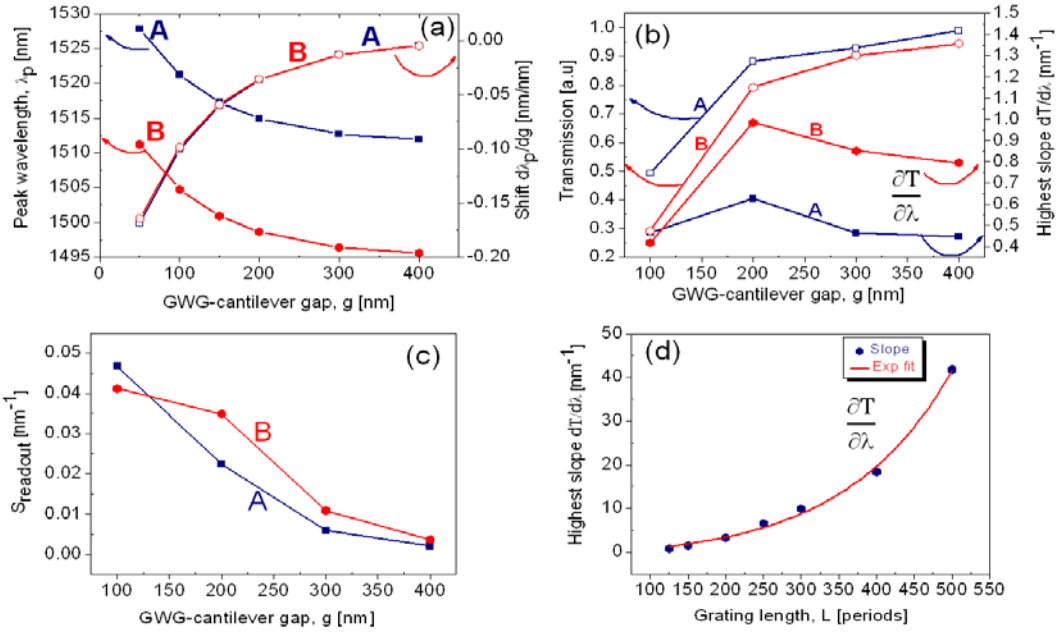

Fig. 2. Device performance with W=20 μm, L=125Λ, and d=55 nm (A) and 75 nm (B): (a) resonant wavelength (left axis) and quantity $\partial\lambda_p/\partial g$ (right axis) versus g, (b) transmission at sharpest peak(left) and highest transmission slope (right) versus g, (c) readout sensitivity $S_{readout}$ versus g, and (d) highest slope versus grating length for device B without a suspended cantilever.

modal field (see Fig. 2a, right axis).We found that this quantity is also nearly independent of grating length, *L* (not shown here).

Figure 2b shows the transmission (left) and the highest slope of the resonant peaks (right) versus different GWG-cantilever gaps. The transmission reduces when the grating is deeper and the GWG-cantilever gap is narrower. The values of the transmission and the highest transmission slope of each device change slightly as a function of the gap size, *g*, except at small gaps (*g*<200 nm). However, the transmission of the deep grating (device B) is slightly lower than that of shallow grating (device A), while the transmission slope of (device B) is higher with a factor 2. The enhancement of the transmission slope of device B leads to a corresponding gain of the readout sensitivity (as shown in Fig. 2c). It is obvious that the deeper grating results in steeper transmission slope, provided that the gap is still large enough (i.e., g>200 nm) and the optical loss remains low. To demonstrate the importance of the grating length we have given in Fig. 2d a graph of $\partial T/\partial\lambda$ versus *L*, showing that the slope increases rapidly with the grating length. In brief, by choosing a proper initial GWG-cantilever gap maintaining a low optical loss, i.e., g>200 nm, the sensitivity and thus the detection limit can be increased significantly with higher Q cavities as a result of deeper or/and longer gratings.

4.2. Fixed *g*=200 nm, varied *L* and *W/L* ratio

In this part, the GWG-cantilever gap and grating depth are fixed at the values of *g=200 nm* and *d=55* nm, respectively. The cantilever width will be varied relatively to the grating length *L=125*Λ (device C) and *L=250*Λ (device D), namely the *W/L* ratio.

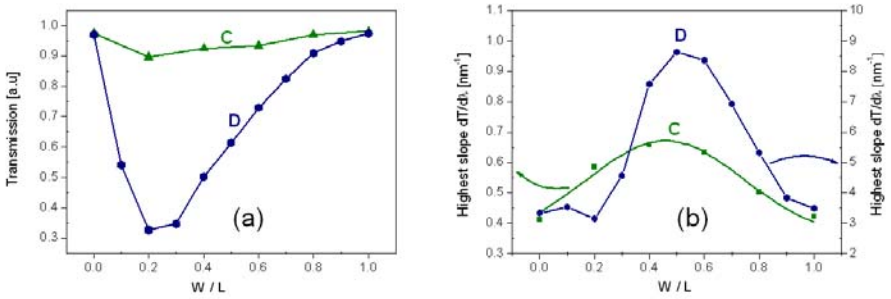

Fig. 3. Transmission (a) and highest transmission slope (b) versus cantilever width/ grating length ratio of device C (L=125Λ) and device D (L=250Λ).

Figure 3a shows the transmittance of both devices versus the *W/L* ratio. Changing the *W/L* ratio from 0 to 1 leads to the transmission drop of maximum 10% and 65% with respect to short and long grating. The highest transmission slope $\partial T/\partial \lambda$ reaches its maximum value around a *W/L* ratio of 0.5, which also corresponds to moderate scattering losses, as shown in Fig. 3b. The results also reconfirm the importance of the grating length as the slope $\partial T/\partial \lambda$ increases by a factor of 12 if the length is increased by a factor of 2.

5. Conclusions

In conclusion, we have demonstrated preliminary results of a numerical investigation and optimization of a novel sensing device based on the integration of a cantilever and a grated waveguide. Such a device can potentially be used for detection of small amount of gas concentration through nano-displacement of the suspended cantilever. Sensor performance dependent on grating length and depth, cantilever width and GWG-cantilever gap are investigated. Increasing grating length or depth at an optimized cantilever width and a proper initial gap results in a high sensitivity and thus low detection limit. However, too long or too deep gratings may lead to a high optical scattering loss, such that the transmittance peaks may get obscured by noise.

Acknowledgements

This research is supported by MEMSland, a project of the Point One program funded by the Ministry of Economic Affairs and the STW Technology Foundation through project TOE. 6596.

References

[1] S.V. Pham, L.J. Kauppinen, M. Dijkstra, H.A.G.M. van Wolferen, R.M. de Ridder and H.J.W.M.Hoekstra, *Read-out of cantilever bending with a grated waveguide optical cavity,* submitted.

[2] S. Okuyama, Y. Mitobe, K. Okuyama, and K. Matsushita, "*Hydrogen gas gensing using a Pd-coated cantilever,"* Jpn. J. Appl. Phys., vol.39, pp. 3584-3590, 2000.

[3] D.R. Baselt, B. Fruhberger, E. Klaassen, S. Cemalovic, C. L. Britton Jr., S.V. Patel, T.E. Mlsna, D. McCorkle, and B. Warmack, "*Design and performance of a microcantilever-based hydrogen sensor,"* Sensors and Actuators B: Chemical, vol. 88, pp. 120-131, 2003.

[4] Z. Hu, T. Thundat, and R.J. Warmack, *"Investigation of adsorption and absorption-induced stresses using microcantilever sensors,"* J. Appl. Phys., vol. **90**, pp. 427–431, 2001.

[5] W.C.L. Hopman, H.J.W.M. Hoekstra, R. Dekker, L. Zhuang, R.M. de Ridder, *"Far-field scattering microscopy applied to analysis of slow light, power enhancement, and delay times in uniform Bragg waveguide gratings,"* Opt. Express, vol. 15, pp. 1851-1870, 2007.

[6] L.J. Kauppinen, H.J.W.M. Hoekstra, M. Dijkstra, R.M. de Ridder, and G.J.M. Krijnen, *"Grated waveguide optical cavity as a compact sensor for sub-nanometre cantilever deflections,"* Proc. 14th European Conference on Integrated Optics (ECIO2008), pp. 111-114, 2008.

[7] John D. Joannopoulos, Steven G. Johnson, Joshua N. Winn, and Robert D. Meade, *"Photonic Crystals: Molding the Flow of Light"* , Princeton University Press, 2nd edition, 2008.